

Distinguishing Heterogeneous and Homogeneous CE Mechanisms: Theoretical Insights into Square-Wave Voltammetry

Valentin Mirceski,* Rubin Gulaboski, and Richard G. Compton



Cite This: <https://doi.org/10.1021/acs.jpcc.2c07298>



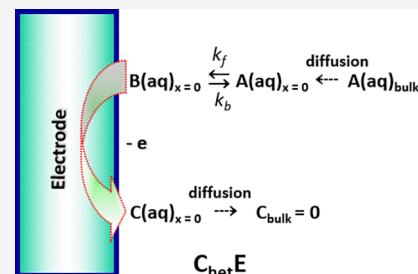
Read Online

ACCESS |

Metrics & More

Article Recommendations

ABSTRACT: A theoretical study of an electrode mechanism where the electrode reaction (E) is preceded by a chemical reaction that takes place solely at the electrode surface (C_{het}) is presented under conditions of square-wave voltammetry (SWV). Rigorous mathematical solutions in the form of integral equations derived by means of Laplace transforms are presented for the surface concentration of all species involved in the electrode mechanism, yielding explicit recurrent formulas for the simulation of the voltammetric response. The theory approximately predicts that the chemical reaction starts at the beginning of the voltammetric experiment, disregarding its occurrence in the short time period between inserting the electrode in the solution until starting the voltammetric experiment. It is demonstrated that SWV can differentiate between the common CE mechanism, where C is a homogeneous chemical reaction taking place in the vicinity of the electrode, and the current $C_{\text{het}}E$ mechanism, which is relevant for plethora of electrocatalytic processes at electrodes modified with catalytically active enzymes and/or noble-metal nanoparticles, as well as for electrocatalytic processes of fundamental importance such as CO_2 , N_2 , O_2 , and H^+ reductions.



1. INTRODUCTION

Studying chemical reactions coupled with electrode processes is one of the main tasks of voltammetry.^{1–3} The theory of voltammetry encompasses a plethora of electrode mechanisms involving chemical reactions, which either precede or follow the electrode reaction, resulting in well-known reaction schemes abbreviated as CE, EC, EC', ECE, and many more, where C is the symbol for a chemical reaction and E signifies an electrode reaction. Commonly, the chemical reaction is assumed to be a homogeneous process taking place in the electrolyte solution in the vicinity of the electrode surface.^{4–7} In some cases, the chemical reaction can be confined to the electrode surface,⁸ as, for instance, in electrode mechanisms coupled with surface complexation,^{9,10} or ion-exchange reactions at surface-modified electrodes.^{11,12} Moreover, in adsorption, complicated electrode mechanisms where the redox species are involved in adsorption equilibrium, the accompanying chemical reaction can be either of surface or volume nature.^{13,14} Specifically, the surface chemical reaction involves adsorbed redox species, whereas the volume chemical reaction is related to the dissolved species. Laviron initiated a remarkable discussion whether these two closely similar, but not identical, chemical reactions can be differentiated.¹³ Later, it has been demonstrated that these two types of chemical reactions can be clearly differentiated under conditions of square-wave voltammetry (SWV) for an adsorption complicated EC mechanism, owing to the notable sensitivity of the technique to the adsorption equilibria.^{15–17}

In the light of contemporary electrochemistry focused on electrode processes at surface-modified electrodes,¹⁸ in

particular electrodes modified with enzymes,^{19,20} and/or nanoparticles,²¹ the intrinsic nature of the accompanying chemical reaction is becoming an important question. The strong catalytic activity of surface-confined enzymes or noble metal nanoparticles prompts chemical reactions taking place at the electrode surface only,^{22,23} which either precede or follow the electrode reaction. A remarkable example is the electrode mechanism of hydrogen peroxide reduction at a carbon electrode modified with noble metal nanoparticles (e.g., silver²⁴ or palladium²⁵), where disproportionation of hydrogen peroxide takes place on the surface of nanoparticles only. Thus, chemically generated oxygen on the electrode surface is the electroactive reactant, completing a $C_{\text{het}}E$ electrode mechanism, where C_{het} designates a heterogeneous chemical reaction preceding the electrode reaction. Hence, the question arises whether $C_{\text{het}}E$ can be differentiated from the conventional CE mechanism under voltammetric conditions. The question is also relevant for other electrocatalytic processes of fundamental importance such as the reduction of CO_2 ,^{26,27} N_2 ,^{28–30} O_2 ,³¹ and H^+ ,³² where electron transfer is frequently preceded by a chemical rearrangement (e.g., chemisorption, complex forma-

Received: October 17, 2022

Revised: January 11, 2023

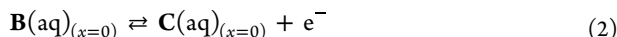
tion, hydration, dehydration, etc.). The aim of the current study is to provide a theoretical background for the simulation of the $C_{\text{het}}E$ mechanism, in order to find specific voltammetric features for differentiation from the common CE reaction scheme. The study is conducted under conditions of SWV³³ applying rigorous mathematical modeling by means of Laplace transforms, for the case of a quasireversible electrode reaction of a dissolved redox couple at a conventional macroscopic planar electrode.

2. MATHEMATICAL MODEL

A chemical reaction taking place at the electrode surface is described with eq 1:



The subscript $x = 0$ designates the distance measured from the electrode surface. It should be emphasized that the preceding chemical reaction takes place only at the distance $x = 0$ (i.e., at the electrode surface), which is the main difference to the common CE scheme, where the chemical reaction takes place in the solution, i.e., at $x \geq 0$. Reaction 1 is characterized with heterogeneous forward (k_f) and backward (k_b) rate constants, both in units of cm s^{-1} , and the equilibrium constant is defined as $K = k_f/k_b$. Chemical reaction 1 is followed by a common quasireversible one-electron electrode reaction 2:



It is assumed that all reactants are soluble in the electrolyte solution and the kinetic equations below are formulated in terms of the solution-phase concentrations immediately adjacent to the electrode, not adsorbed concentrations, although for weak adsorption of A, the distinction is academic since the adsorbed concentrations will be proportional to the local solution phase concentration.³⁴ Equally for the case when the adsorbed species reacts quickly so that the steady-state coverage is negligible, the assumed kinetics will apply, and a pre-equilibrium operates prior to the overall rate-determining electron transfer. The mass transport is described by the following differential equation:

$$\frac{\partial c_i}{\partial t} = D \frac{\partial^2 c_i}{\partial x^2} \quad (3)$$

valid for any of the species in eqs 1–2. Initially, only the reactant A is present in the solution. Thus, the boundary value problem is defined as follows:

$$t = 0, x \geq 0: c_A = c_A^*, c_B = c_C = 0 \quad (4)$$

$$t > 0, x \rightarrow \infty: c_A \rightarrow c_A^*, c_B = c_C \rightarrow 0 \quad (5)$$

$$t > 0, x = 0: D \left(\frac{\partial c_A}{\partial x} \right)_{x=0} = k_f(c_A)_{x=0} - k_b(c_B)_{x=0} \quad (6)$$

The boundary conditions 4–6 assume that the chemical reaction did not take place prior to the voltammetric experiment. In a rigorous discussion, the chemical reaction starts as soon as the electrode is brought in contact with the solution. In the time period between inserting the electrode, positioning in the solution, and starting the voltammetric experiment, some surface concentrations of A and B species are established, which slightly deviates from the values defined in eq 4, but they are difficult to be predicted. Thus, condition 4 is a necessary approximation for consistent mathematical treatment by means of Laplace transforms. In addition, it may be worth pointing out

that the initial conditions 4–6 assumed are realized when the chemical reaction is a photo-chemical one so that the chemistry starts once the light is switched on and not before. This is relevant to the extensive work on solar energy. In addition, at the electrode surface, the following conditions hold

$$t > 0, x = 0: D \left(\frac{\partial c_B}{\partial x} \right)_{x=0} = \frac{I}{FS} - k_f(c_A)_{x=0} + k_b(c_B)_{x=0} \quad (7)$$

$$t > 0, x = 0: D \left(\frac{\partial c_C}{\partial x} \right)_{x=0} = -\frac{I}{FS} \quad (8)$$

For the sake of simplicity, the model assumes an identical diffusion coefficient for all dissolved species. However, the model is not constrained by this assumption and it can be easily adopted for different values of the diffusion coefficient of each diffusion species. The conditions at the electrode surface are additionally defined by the Butler–Volmer equation:

$$\frac{I}{FS} = k_s \exp(\beta\phi) [(c_B)_{x=0} - (c_C)_{x=0} \exp(-\phi)] \quad (9)$$

Here, $\phi = F(E - E^0)/RT$ is dimensionless electrode potential, I is the current, S is the electrode surface area, F is the Faraday constant, β is the electron transfer coefficient, c_A^* is the bulk concentration of the reactant A, and D is the common diffusion coefficient.

The solutions for the surface concentrations of species A, B, and C in the Laplace domain read:

$$\mathfrak{F}(c_A)_{x=0} = \frac{b}{\sqrt{s} + a} \mathfrak{F}(c_B)_{x=0} + \frac{c_A^*}{\sqrt{s}(\sqrt{s} + a)} \quad (10)$$

where \mathfrak{F} is the symbol for the Laplace transform, s is Laplace variable, $b = \frac{k_b}{\sqrt{D}}$, and $a = \frac{k_f}{\sqrt{D}}$.

$$\mathfrak{F}(c_B)_{x=0} = \frac{ac_A^*}{s(\sqrt{s} + c)} - \frac{1}{\sqrt{s} + c} \frac{\mathfrak{F}I}{FS\sqrt{D}} - \frac{1}{\sqrt{s}(\sqrt{s} + c)} \frac{\mathfrak{F}I}{FS\sqrt{D}} \quad (11)$$

where $c = a + b$.

$$\mathfrak{F}(c_C)_{x=0} = \frac{1}{\sqrt{s}} \frac{\mathfrak{F}I}{FS\sqrt{D}} \quad (12)$$

The solutions for the surface concentration of B and C in time domain are as follows:

$$(c_B)_{x=0} = \frac{ac_A^*}{c} [1 - \exp(c^2t) \text{erfc}(c\sqrt{t})] - \int_0^t \frac{I(\tau)}{FS\sqrt{D}} \frac{d\tau}{\sqrt{\pi(t-\tau)}} + (c-a) \int_0^t \frac{I(\tau)}{FS\sqrt{D}} \exp[c^2(t-\tau)] \text{erfc}(c\sqrt{t-\tau}) d\tau \quad (13)$$

$$(c_C)_{x=0} = \int_0^t \frac{I(\tau)}{FS\sqrt{D}} \frac{d\tau}{\sqrt{\pi(t-\tau)}} \quad (14)$$

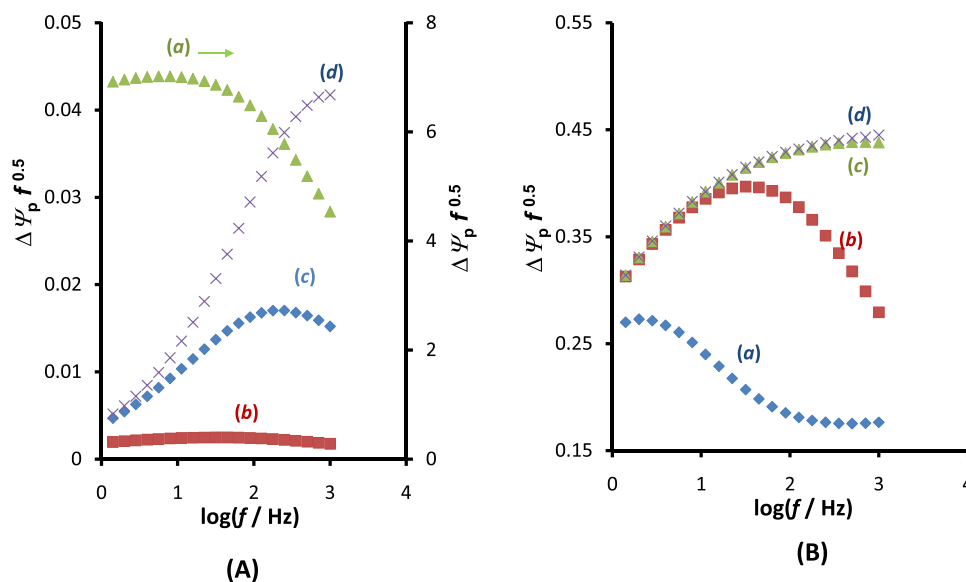


Figure 1. Effect of the frequency on the real net peak-current calculated for (A) different kinetics of the chemical reaction and (B) different electrode kinetics. For (A) the cumulative chemical rate constant $\epsilon = k_f + k_b$ is $\log(\epsilon) = -5$ (a); -4 (b); -3 (c), and -2.4 (d). Standard rate constant is $k_s = 0.01 \text{ cm s}^{-1}$, while the magnitude of the diffusion coefficient is $D = 1 \times 10^{-6} \text{ cm}^2 \text{ s}^{-1}$. Curves (b) and (c) refer to the right ordinate. For (B), the standard rate constant is $\log(k_s / \text{cm s}^{-1}) = -3$ (a); -2 (b); -1 (c), and 0 (d), for $\log(\epsilon) = -4$. The other conditions are as follows: equilibrium constant $K = 100$, electron transfer coefficient $\beta = 0.5$, SW amplitude $E_{sw} = 50 \text{ mV}$, temperature $T = 298.15 \text{ K}$, and step potential $\Delta E = 10 \text{ mV}$.

The recurrent formula for the simulation of the experiment under conditions of SWV reads:

$$\Psi_m = \frac{\kappa \exp(\beta\phi_m) \left[\frac{a}{c} \left(1 - \exp\left(\frac{\lambda^2 m}{50}\right) \operatorname{erfc}\left(\lambda \sqrt{\frac{m}{50}}\right) \right) - \frac{2(1 + \exp(-\phi))}{\sqrt{50\pi}} \sum_{j=1}^{m-1} \Psi_j S_{m-j+1} + \left(\frac{c-a}{c}\right) \sum_{j=1}^{m-1} \Psi_j R_{m-j+1} \right]}{1 - \kappa \exp(\beta\phi_m) \left[-\frac{2(1 + \exp(-\phi))}{\sqrt{50\pi}} + \frac{c-a}{c} R_1 \right]} \quad (15)$$

Here $\lambda = \frac{\epsilon}{\sqrt{Df}}$ is the dimensionless chemical kinetic parameter, where $\epsilon = k_f + k_b$ is the cumulative rate constant, while $\kappa = \frac{k_s}{\sqrt{Df}}$ is the dimensionless electrode kinetic parameter. Note that $a/c =$

$K/(K+1)$ and $(c-a)/c = 1/(K+1)$, where $K = k_f/k_b$ is equilibrium constant. Thus, the recurrent formula 15 is rewritten as

$$\Psi_m = \frac{\kappa \exp(\beta\phi_m) \left[\frac{K}{K+1} \left(1 - \exp\left(\frac{\lambda^2 m}{50}\right) \operatorname{erfc}\left(\lambda \sqrt{\frac{m}{50}}\right) \right) - \frac{2(1 + \exp(-\phi))}{\sqrt{50\pi}} \sum_{j=1}^{m-1} \Psi_j S_{m-j+1} + \left(\frac{1}{K+1}\right) \sum_{j=1}^{m-1} \Psi_j R_{m-j+1} \right]}{1 - \kappa \exp(\beta\phi_m) \left[-\frac{2(1 + \exp(-\phi))}{\sqrt{50\pi}} + \frac{1}{K+1} R_1 \right]} \quad (16)$$

In eqs 15 and 16

$$R_m = \frac{2\sqrt{m}}{\sqrt{50\pi}} - \frac{1}{\lambda} \left[1 - \exp\left(\frac{\lambda^2 m}{50}\right) \operatorname{erfc}\left(\lambda \sqrt{\frac{m}{50}}\right) \right] - \left\{ \frac{2\sqrt{m-1}}{\sqrt{50\pi}} - \frac{1}{\lambda} \left[1 - \exp\left(\frac{\lambda^2(m-1)}{50}\right) \operatorname{erfc}\left(\lambda \sqrt{\frac{m-1}{50}}\right) \right] \right\}$$

$S_m = m^{1/2} - (m-1)^{1/2}$ are numerical integration parameters. $\Psi = I(FSc_A^*)^{-1}(Df)^{-1/2}$ is the dimensionless current, where f is the SW frequency and m is the serial number of time increments. The time increment is defined as $\Delta t = 1/(50f)$, i.e., each potential pulse is divided into 25 time increments.³³ All

simulations have been performed by the commercial package MATHCAD 14.

3. RESULTS AND DISCUSSION

Voltammetric characteristics of the $C_{het}E$ mechanism depend predominantly on the dimensionless chemical kinetic parameter λ , the equilibrium constant K , and the dimensionless electrode kinetic parameter κ . The physical meaning of K and κ are well-known from the previous theory of the conventional CE reaction scheme^{17,33,35-37} as well as from the theory of a simple quasireversible electrode reaction.³³ Briefly, the equilibrium constant K determines the concentration ratio of A and B species (eq 1) at the electrode surface in the state of equilibrium, whereas the electrode kinetic parameter κ controls predominantly the electrochemical reversibility of the electrode reaction (eq 2). The dimensionless chemical kinetic parameter $\lambda = \frac{\epsilon}{\sqrt{Df}}$

represents the cumulative rate constant of the preceding chemical step $\varepsilon = k_f + k_b$ (eq 1), relative to the diffusion rate constant (D) and the critical time of the voltammetric experiment (f), i.e., the product \sqrt{Df} . We note that the parameter \sqrt{Df} with units cm s^{-1} is different to the common chronoamperometric parameter \sqrt{Dt} (cm) that represents the diffusion layer thickness. The parameter \sqrt{Df} (cm s^{-1}) could be provisionally understood as a diffusional rate constant, which, relative to the electron transfer rate constant k_s (in the electrode kinetic parameter $\kappa = \frac{k_s}{\sqrt{Df}}$) and the cumulative chemical rate constant $\varepsilon = k_f + k_b$ (in the chemical kinetic parameter $\lambda = \frac{\varepsilon}{\sqrt{Df}}$), reveals the intrinsic role of both electron transfer and the chemical reaction. Therefore, the rate of diffusion is critically important for the chemical step and the electrode reaction, as both take place at the electrode surface only. Recall that in the conventional CE mechanism,^{17,35–37} the chemical parameter is defined as $\lambda = \frac{\varepsilon}{f}$, where the cumulative rate constant ε is presented relative to the critical time of the voltammetric experiment only (i.e., the SW frequency, f) as the rate of diffusion is insignificant for the chemical reaction.

The morphology of the voltammetric response (i.e., shape, peak current ratio, and relative position of the forward and backward SW components) depend predominantly on the electrode reaction (eq 2) and the electrode kinetic parameter κ . Studying the effect of λ , while keeping other parameters constant, one finds a sigmoid-like dependence of the net peak current ($\Delta\Psi_p$) vs $\log(\lambda)$ over the interval $-3 \leq \log(\lambda) \leq 1$. The intensity of the voltammetric response increases in proportion to the rate of the preceding chemical reaction, as the chemical reaction generates more of the electroactive reactant **B** on the electrode surface. A particular shape of the function $\Delta\Psi_p$ vs $\log(\lambda)$ depends on K and κ , which is very similar to the conventional CE mechanism;^{17,35–37} thus, such analysis does not provide a basis to reveal the nature of the preceding chemical reaction. Correspondingly, the functions $\Delta\Psi_p$ vs $\log(K)$ and $\Delta\Psi_p$ vs $\log(\kappa)$ are sigmoid, and their characteristics are known from the theory of the conventional CE mechanism.^{17,35–37}

Let us note that independent variation of any of these parameters (λ , K , or κ) corresponds to a comparison of a series of different reactions, rather than to the analysis of a single electrode mechanism that is characterized with a unique set of constants. Hence, in studying a single electrode mechanism, dimensionless parameters can be altered by varying the frequency of the potential modulation. A set of simulations corresponding to the analysis of a single experimental system are summarized in Figure 1, where the effect of the SW frequency to the product $\Delta\Psi_p\sqrt{f}$ is presented. Note that the product $\Delta\Psi_p\sqrt{f}$ corresponds to the real net-peak current (ΔI_p), which can be experimentally measured. As shown in Figure 1, the real net-peak current is a parabolic function on $\log(f)$ for different values of the cumulative rate constant $\varepsilon = k_f + k_b$ and the standard rate constant (k_s). Such a specific effect of the frequency is typical for the current mechanism and was not found for the conventional CE mechanism.^{17,35–37} The origin of such a voltammetric feature stems from the complex simultaneous influence of the frequency to the rates of the chemical reaction, electron transfer, and diffusion. An increase in the frequency means a shorter period available for the chemical reaction to take place; on the other hand, the thickness of the diffusion layer generally

diminishes by increasing the frequency, causing faster diffusion, which increases the overall rate of the chemical step. Thus, the interplay of these two opposite effects (shorter time for chemical reaction but faster diffusion) results in a parabolic dependence of the real net-peak current on the SW frequency. The maximum of the parabolic function presented in Figure 1 depends on the specific value of the cumulative rate constant ε and the standard rate constant k_s . Generally, the maximum is positioned at a higher frequency for a faster chemical reaction (Figure 1A) and a faster electrode reaction (Figure 1B). Let us additionally note that a parabolic dependence of the real net-peak current on the SW frequency is not predicted so far for any electrode mechanism of a dissolved redox couple in the theory of SWV.³³

Another peculiar voltammetric feature of the studied mechanism is the effect of the initial potential of the voltammetric experiment, which is presented in Figure 2. Considering the

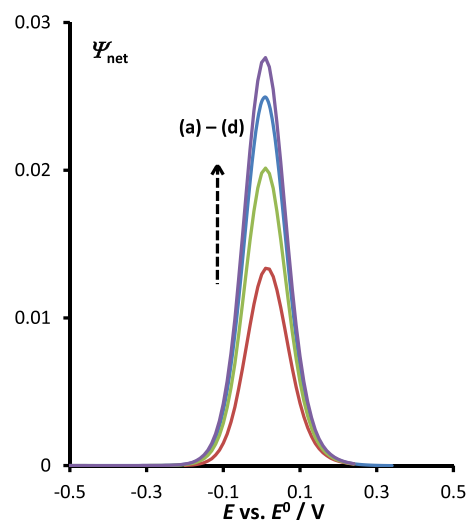


Figure 2. Effect of the starting potential (E_s vs E^0) on the net SW voltammograms. The values of the starting potentials in the direction of the arrow given on the plot are $E_s/V = -0.200$ (a); -0.500 (b); -0.800 (c) and -1.000 (d). The other conditions of the simulations are chemical kinetic parameter $\log(\lambda) = -2.0$, equilibrium constant $K = 1$, electrode kinetic parameter $\log(\kappa) = -0.075$, electron transfer coefficient $\beta = 0.5$, SW amplitude $E_{sw} = 50$ mV, and step potential $\Delta E = 10$ mV.

initial conditions assumed in the theoretical model (eq 4), the voltammetric experiment and thus the chemical reaction start as soon as the electrode is inserted into the electrolyte solution. Consequently, the initial potential value relative to the formal potential of the electrode reaction determines the time for the chemical reaction to take place prior to the electrode reaction. Theoretical net SW voltammograms in Figure 2 clearly reveal such an effect. The same voltammetric behavior can be observed by conditioning the electrode for a certain time period prior application of the potential modulation. The intensity of the response (i.e., the net peak-current) increases in proportion to the square-root of the conditioning time, reflecting the effect of the diffusional mass transport of the initial reactant **A** (eq 1) to the electrode surface. As well-known, analogous voltammetric behavior can be found in electrode processes affected by the adsorption of the reactant, where the adsorptive accumulation enlarges the voltammetric response. However, in adsorption-coupled processes, a narrow stripping net SW peak emerges, reflecting the surface electrode reaction of the electroactive

reactant.³³ In the present system however, the morphology of all SW voltammetric components reflects diffusion-affected electrode reaction, while the real net-peak current is a parabolic function of the frequency, providing a clear means for the differentiation of the heterogeneous nature of the preceding chemical reaction.

If the chemical reaction is in equilibrium at the beginning of the experiment (i.e., at $t = 0$; $x \geq 0$), both species A and B are present initially in the solution at their equilibrium concentrations (c_A^* and c_B^*). They are related through the equilibrium constant $K = \frac{c_B^*}{c_A^*}$ and their sum defines the initial total concentration $c_A^* + c_B^* = c^*$. Under such conditions, the solution for the surface concentration of B species reads

$$(c_B)_{x=0} = \frac{ac_A^*}{c} [1 - e^{c^2 t} (\operatorname{erfc}(c\sqrt{t})) + c_B^* \left[\frac{a}{c} + \left(1 - \frac{a}{c}\right) e^{c^2 t} \operatorname{erfc}(c\sqrt{t}) \right] - \int_0^t \frac{I(\tau)}{FS\sqrt{D}} \frac{d\tau}{\sqrt{\pi(t-\tau)}} + (c-a) \int_0^t \frac{I(\tau)}{FS\sqrt{D}} e^{c^2(t-\tau)} \operatorname{erfc}(c\sqrt{t-\tau}) d\tau \quad (17)$$

Simulations conducted by taking into account the latter equation have shown that the effect illustrated in Figure 2 is absent and the intensity of the response does not depend on the initial potential and the preconditioning time. However, it is interesting to compare the effect of the equilibrium constant for the case when the experiment starts only with the reactant A and when both reactants A and B are present in a chemical equilibrium at the beginning of the experiment. Figure 3 summarizes such analysis for the same kinetics of the chemical reaction and for the typical quasireversible electrode reaction.

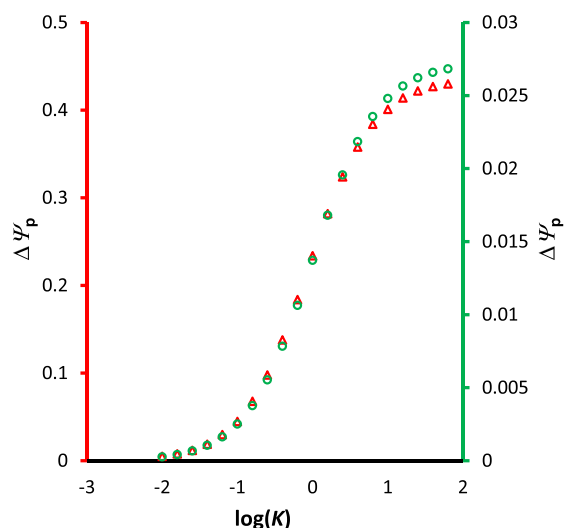


Figure 3. Effect of the equilibrium constant on the net peak-current when the experiment starts with the reactant A present in the solution only (circles, right ordinate) and with equilibrium concentrations of both A and B species (triangles, left ordinate). The chemical kinetic parameter is $\log(\lambda) = -1$, electrode kinetic parameter $\log(\kappa) = -0.5$, electron transfer coefficient $\beta = 0.5$, step potential $\Delta E = 5$ mV, and the starting potential is $E_s = -0.200$ vs E^0 .

Clearly, the effect of the equilibrium constant is identical in both cases, the only difference is in the absolute values of the currents. More importantly, when the equilibrium is established prior to the voltammetric experiment, the parabolic relation between the net peak-current and the frequency vanishes, and the overall voltammetric behavior strongly resembles the common CE mechanism.

Considering the complexity of the studied model, it is of particular interest to find voltammetric features which depend solely on either the chemical or the electrode reaction, in order to develop a strategy for unambiguous estimation of the critical kinetic parameters. To this goal, the role of the SW amplitude (E_{sw}) is studied in analyzing the voltammetric data. As previously demonstrated,³⁸ studying a particular mechanism by altering the SW amplitude at a given frequency is advantageous as the frequency-dependent dimensionless kinetic parameters are constant in the course of the analysis, and the voltammetric behavior is simple. The effect of the amplitude is mainly manifested through the influence on the electrode kinetics; thus, it is expected to provide information regarding the electrochemical standard rate constant mainly.

These expectations are confirmed by the data shown in Figure 4, where the amplitude-based quasireversible maximum is

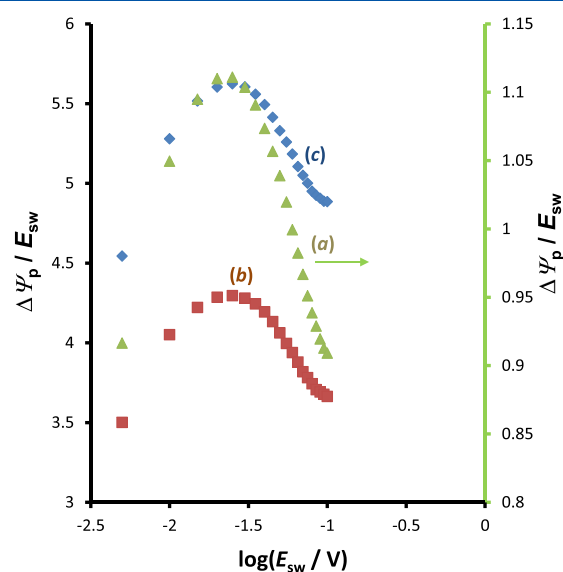


Figure 4. Effect of the amplitude on the amplitude-normalized net peak-current for different kinetics of the chemical reaction. The chemical kinetic parameter is $\log(\lambda) = -1.5$ (a); -0.5 (b); and 1.5 (c). Other conditions are equilibrium constant $K = 100$, electrode kinetic parameter $\log(\kappa) = -1$, electron transfer coefficient $\beta = 0.5$, and step potential $\Delta E = 10$ mV. Curve (a) refers to the right ordinate.

studied for different rate constants of the chemical reaction. Let us recall that the amplitude-based quasireversible maximum is a general feature of diffusion-affected electrode processes where the amplitude-normalized net peak current is studied as a function of the SW amplitude.³⁸ Commonly, a parabolic function is obtained, the position of which solely depends on the standard rate constant. The data in Figure 4 reveal that the position of the maximum is unaffected by the rate of the preceding chemical reaction, thus enabling unambiguous determination of the standard rate constant (k_s), without previous knowledge of the chemical rate constant.

4. CONCLUSIONS

Consistent with previous findings,^{15–17} SWV can uncover subtle differences in very similar electrode mechanisms, particularly when the electrode reaction is coupled with adsorption equilibria and/or chemical reactions. To the best of our knowledge, it is the first theoretical study of the specific $C_{\text{het}}E$ mechanism based on Laplace transforms, which provide solutions for surface concentrations of all involved species. Rigorously speaking, it is plausible to assume that the preceding chemical reaction takes place via the adsorbed state of the relevant species, requiring account be taken of the adsorption equilibria of all species. However, under such a scenario, the model will not be mathematically tractable with Laplace transforms and fully numerical approach in mathematical modeling will be required. Some of the characteristic voltammetric features of the present model are the parabolic dependence of the real net peak current on the SW frequency and the effect of the initial potential.

Rigorous mathematical solutions of the current mechanism are not identical with the CE case, clearly indicating that both cases are not identical and the overall study is not trivial. When the equilibrium is assumed at the beginning of the experiment (eq 17), the voltammetric behavior is only qualitatively identical to the common CE reaction scheme; however, it does not mean that quantitative analysis of the $C_{\text{het}}E$ reaction (with and without equilibrium) can be correctly done with the common CE model. Rigorously speaking, the initial condition 4, which assumes the chemical reaction to start simultaneously with the voltammetric experiment, is an approximation, as the chemical reaction takes place as soon as the electrode is brought into contact with the solution. The real surface concentrations of A and B species formed since inserting the electrode, positioning, and starting the voltammetric experiment are difficult to be predicted. Such an approximation is a prerequisite for the mathematical treatment of the electrode mechanisms with Laplace transforms.

The current model can be easily adopted for any voltammetric and/or chronoamperometric technique. Considering the theory of SWV, it is the first electrode mechanism of dissolved species in which the real net-pet current parabolically depends on the logarithm of the frequency, providing a means for qualitatively differentiating the $C_{\text{het}}E$ from the common CE mechanism. In spite of the fact that all species are dissolved in the solution, and thus the response obviously depends on the diffusional mass transfer in the course of voltammetry, the net peak current increases linearly with the square-root of the incubation time of the working electrode in the solution prior the application of the potential variation. This is another specific voltammetric feature enabling clear differentiation from the common CE mechanism. Importantly, features of the voltammetric response exist that are solely sensitive to the electrode kinetics, as the amplitude-based quasireversible maximum,³⁸ which enables to develop a reliable and sequential methodology for full kinetic characterization of the electrode mechanism.

AUTHOR INFORMATION

Corresponding Author

Valentin Mirceski – Department of Inorganic and Analytical Chemistry, University of Lodz, 91-403 Lodz, Poland; Institute of Chemistry, Faculty of Natural Sciences and Mathematics, “Ss Cyril and Methodius” University in Skopje, 1000 Skopje, Republic of North Macedonia; Research Center for Environment and Materials, Macedonian Academy of Sciences

and Arts, 1000 Skopje, Republic of North Macedonia;
orcid.org/0000-0002-9191-3926;
Email: valentin.mircheski@chemia.uni.lodz.pl

Authors

Rubin Gulaboski – Faculty of Medical Sciences, Goce Delcev University, 2000 Stip, Republic of North Macedonia

Richard G. Compton – Department of Chemistry, Physical and Theoretical Chemistry Laboratory, Oxford University, Oxford OX1 3QZ, Great Britain; orcid.org/0000-0001-9841-5041

Complete contact information is available at:
<https://pubs.acs.org/10.1021/acs.jpcc.2c07298>

Notes

The authors declare no competing financial interest.

ACKNOWLEDGMENTS

V.M. acknowledges with gratitude the support from the National Science Centre of Poland through the Opus Lap project no. 2020/39/I/ST4/01854.

REFERENCES

- (1) Compton, R. G.; Laborda, E.; Ward, K. R. Simulation of Electrode Processes. In *Understanding Voltammetry*; Imperial College Press; Dist. by World Scientific, 2014; pp 17–19.
- (2) Savéant, J. M. Elements of molecular and biomolecular electrochemistry: an electrochemical approach to electron transfer chemistry; John Wiley & Sons: Hoboken, New Jersey, 2006.
- (3) Batchelor-McAuley, C.; Kätelhön, E.; Barnes, E. O.; Compton, R. G.; Laborda, E.; Molina, A. Recent advances in voltammetry. *ChemistryOpen* **2015**, *4*, 224–260.
- (4) Amatore, C.; Savéant, J. M.; Thiebault, A. Electrochemically induced chemical reactions kinetics of competition with electron transfers. *J. Electroanal. Chem.* **1979**, *103*, 303–320.
- (5) Amatore, C.; Lexa, D.; Savéant, J. M. ECE reaction pathways in the electrochemical reduction of dicyanocobalamin kinetics of ligand substitution in vitamin b12r cyanocob(ii)alamin. *J. Electroanal. Chem.* **1980**, *111*, 81–89.
- (6) Amatore, C.; Savéant, J. M. Mechanism analysis of electrochemical reactions involving homogeneous chemical steps. The electrodimmerization of 4-methoxybiphenyl. *J. Electroanal. Chem.* **1983**, *144*, 59.
- (7) Amatore, C.; Gareil, M.; Savéant, J. M. Homogeneous vs. heterogeneous electron transfer in electrochemical reactions application to the electrohydrogenation of anthracene and related reactions. *J. Electroanal. Chem.* **1983**, *147*, 1–38.
- (8) Laviron, E.; Electrochemical reactions with protonations at equilibrium. In *Electroanalytical Chemistry*; Bard, A. J., Ed.; Marcel Dekker: New York, 1982; Vol. 12, p 53.
- (9) Sykut, K.; Dalmata, G.; Nowicka, B.; Saba, J. Acceleration of electrode processes by organic compounds – “cap-pair” effect. *J. Electroanal. Chem.* **1978**, *90*, 299–302.
- (10) Souto, R. M.; Sluyters-Rehbach, M.; Sluyters, J. H. On the catalytic effect of thiourea on the electrochemical reduction of cadmium(II) ions at DME from aqueous 1 M KF solutions. *J. Electroanal. Chem.* **1986**, *201*, 33–45.
- (11) Navrátilová, Z.; Kula, P. Cation and anion exchange on clay modified electrodes. *J. Solid State Electrochem.* **2000**, *4*, 342–347.
- (12) Su, Z.; Kole, S.; Harden, L. C.; Palakkal, V. M.; Kim, C. O.; Nair, G.; Arges, C. G.; Renner, J. N. Peptide-Modified Electrode Surfaces for Promoting Anion Exchange Ionomer Microphase Separation and Ionic Conductivity. *ACS Mater. Lett.* **2019**, *1*, 467–475.
- (13) Laviron, E. EC_{irr} reaction with adsorption of the reactants. Surface or homogeneous chemical reaction? *J. Electroanal. Chem.* **1995**, *391*, 187–197.

- (14) Meunier-Prest, R.; Laviron, E. The E-DIM reaction with adsorption of the reactants. Surface vs. volume chemical reaction. *J. Electroanal. Chem.* **1997**, *43*, 61–66.
- (15) Mirceski, V. Square-wave voltammetry of an EC reaction of a partly adsorbed redox couple. *J. Electroanal. Chem.* **2001**, *508*, 138–149.
- (16) Mirceski, V.; Lovric, M. EC Mechanism of an Adsorbed Redox Couple. Volume vs Surface Chemical Reaction. *J. Electroanal. Chem.* **2004**, *565*, 191–202.
- (17) Molina, A.; González, J. Pulse voltammetry in physical electrochemistry and electroanalysis: Theory and applications. In *Monographs in electrochemistry*, Scholz, F., Ed.; Springer, 2016.
- (18) Murray, R. W. Modified electrodes. Chemically modified electrodes for electrocatalysis. *Philos. Trans. R. Soc., A* **1981**, *302*, 253–265.
- (19) Sepunaru, L.; Laborda, E.; Compton, R. G. Catalase-Modified Carbon Electrodes: Persuading oxygen to accept four electrons rather than two. *Chem. – Eur. J.* **2016**, *22*, 5904–5908.
- (20) Le, H.; Compton, R. G. Electrochemical processes mediated via adsorbed Enzymes: Flat and porous electrodes Compared. Understanding Nano-confinement. *J. Electroanal. Chem.* **2021**, *895*, No. 115448.
- (21) Saha, K.; Agasti, S. S.; Kim, C.; Li, X.; Rotello, V. M. Gold Nanoparticles in chemical and biological sensing. *Chem. Rev.* **2012**, *112*, 2739–2779.
- (22) Laborda, E.; Neumann, C. C. M.; Wang, Y.; Ward, K. R.; Molina, A.; Compton, R. G. Heterogeneous Catalysis of Multiple-Electron-Transfer Reactions at Nanoparticle-Modified Electrodes. *ChemElectroChem* **2014**, *1*, 909–916.
- (23) Neumann, C. C. M.; Laborda, E.; Tschulik, K.; Ward, K. R.; Compton, R. G. Performance of silver nanoparticles in the catalysis of the oxygen reduction reaction in neutral media: Efficiency limitation due to hydrogen peroxide escape. *Nano Res.* **2013**, *6*, 511–524.
- (24) Cai, X.; Tanner, E. E. L.; Lin, C.; Ngamchuea, K.; Foord, J. S.; Compton, R. G. The Mechanism of Electrochemical Reduction of Hydrogen Peroxide on Silver Nanoparticles. *Phys. Chem. Chem. Phys.* **2017**, *20*, 1608–1614.
- (25) Čović, J.; Mirceski, V.; Zarubica, A.; Enke, D.; Carstens, S.; Bojić, A.; Randelović, M. Palladium-graphene hybrid as an electrocatalyst for hydrogen peroxide reduction. *Appl. Surf. Sci.* **2022**, *574*, No. 151633.
- (26) Zhang, X.; Guo, S.-X.; Gandionco, K. A.; Bond, A. M.; Zhang, J. Electrocatalytic carbon dioxide reduction: from fundamental principles to catalyst design. *Mater. Today Adv.* **2020**, *7*, No. 100074.
- (27) Amos, P. I.; Louis, H.; Adegoke, K. A.; Eno, E. A.; Udochukwu, A. O.; Magu, T. O. Understanding the Mechanism of Electrochemical Reduction of CO₂ Using Cu/Cu-Based Electrodes: A Review. *Asian J. Nanosci. Mater.* **2018**, *1*, 183–224.
- (28) Tayyebi, E.; Abghoui, Y.; Skúlason, E. Elucidating the Mechanism of Electrochemical N₂ Reduction at the Ru(0001) Electrode. *ACS Catal.* **2019**, *9*, 11137–11145.
- (29) Guo, X.; Yi, W.; Qu, F.; Lu, L. New insights into mechanisms on electrochemical N₂ reduction reaction driven by efficient zero-valence Cu nanoparticles. *J. Power Sources* **2020**, *448*, No. 227417.
- (30) Kaiprathu, A.; Velayudham, P.; Teller, H.; Schechter, A. Mechanisms of electrochemical nitrogen gas reduction to ammonia under ambient conditions: a focused review. *J. Solid State Electrochem.* **2022**, *26*, 1.
- (31) Zhao, Z.; Shen, P.K.; Mechanism of Oxygen Reduction Reaction. In *Electrochemical Oxygen Reduction. Fundamental and Applications*, Shen, P. K., Ed.; Springer: Singapore, 2021; pp 11–27.
- (32) Liang, Z.; Ahn, H. S.; Bard, A. J. A Study of the Mechanism of the Hydrogen Evolution Reaction on Nickel by Surface Interrogation Scanning Electrochemical Microscopy. *J. Am. Chem. Soc.* **2017**, *139*, 4854–4858.
- (33) Mirceski, V.; Komorsky-Lovric, S.; Lovric, M. Square-wave voltammetry: Theory and applications. In *Monographs in electrochemistry*; Scholz, F., Ed.; Springer, 2007.
- (34) Janda, D. C.; Barma, K.; Kurapati, N.; Klymenko, O. V.; Oleinick, A.; Svir, I.; Amatore, C.; Amemiya, S. Systematic assessment of adsorption-coupled electron transfer toward voltammetric discrimination between concerted and non-concerted mechanisms. *Electrochim. Acta* **2022**, *428*, No. 140912.
- (35) Osteryoung, J. G.; O’Dea, J. J. Square-Wave Voltammetry. In *Electroanalytical chemistry: a series of advances*, Bard, A. J. Ed.; Marcel Dekker, 1986; Vol. 14, p 209.
- (36) Osteryoung, J. G.; O’Dea, J. J.; Osteryoung, R. A. Theory of square-wave voltammetry for kinetic systems. *Anal. Chem.* **1981**, *53*, 695–701.
- (37) Garay, F.; Lovric, M. Square-wave voltammetry of quasi-reversible electrode processes with coupled homogeneous chemical reactions. *J. Electroanal. Chem.* **2002**, *518*, 91–102.
- (38) Mirceski, V.; Laborda, E.; Guziejewski, D.; Compton, R. G. New approach to electrode kinetic measurements in square-wave voltammetry: amplitude-based quasireversible maximum. *Anal. Chem.* **2013**, *85*, 5586–5594.